

# PEARL: Data Synthesis via Private Embeddings and Adversarial Reconstruction Learning

Seng Pei Liew, Tsubasa Takahashi, Michihiko Ueno

LINE Corporation

{sengpei.liew,tsubasa.takahashi,michihiko.ueno}@linecorp.com

## Abstract

We propose a new framework of synthesizing data using deep generative models in a differentially private manner. Within our framework, sensitive data are sanitized with rigorous privacy guarantees in a one-shot fashion, such that training deep generative models is possible without re-using the original data. Hence, no extra privacy costs or model constraints are incurred, in contrast to popular approaches such as Differentially Private Stochastic Gradient Descent (DP-SGD), which, among other issues, causes degradation in privacy guarantees as the training iteration increases. We demonstrate a realization of our framework by making use of the characteristic function and an adversarial re-weighting objective, which are of independent interest as well. Our proposal has theoretical guarantees of performance, and empirical evaluations on multiple datasets show that our approach outperforms other methods at reasonable levels of privacy.

## 1 Introduction

Synthesizing data under differential privacy (DP) [11–13] enables us to share the synthetic data and generative model with rigorous privacy guarantees. Particularly, DP approaches of data synthesis involving the use of deep generative models have received attention lately [40, 47, 42, 15, 49, 7, 18].

Typically, the training of such models utilizes a technique called Differentially Private Stochastic Gradient Descent (DP-SGD) to preserve privacy [1]. Roughly speaking, DP-SGD proceeds as follows: (1) sample a random batch of data, (2) calculate and clip the gradients, (3) sanitize the gradients by adding noise. While DP-SGD is a powerful technique enabling deep learning with DP, due to composability, each access to data leads to degradation in privacy guarantees, and as a result, the training iteration is limited by the privacy budget. Most DP-SGD based works are only able to produce usable image data at a rather low level of privacy, i.e.,  $\epsilon \simeq 10$  [47, 42, 7]. Furthermore, DP-SGD often requires extensive hyperparameter search for the optimal clipping size, which is not trivial as small clipping can destroy gradient information, while relaxed clipping can be too noisy for training.

In this work, we seek a strategy of training deep generative models privately alternative to DP-SGD that is free of the aforementioned shortcomings, and is practical in terms of privacy (e.g., usable image data at  $\epsilon \simeq 1$ .)

We propose a general framework called **PEARL** (Private Embeddings and Adversarial Reconstruction Learning). In this framework, the sensitive training data are (1) projected to an informative embedding in a DP manner. (2) The sensitive data may be accessed again for obtaining (private) auxiliary information (e.g., class distribution/proportion for training with imbalanced data) useful for training, but the training of the generative model is restricted to this limited number of accesses to establish strong privacy guarantees. (3) Then, the generative model is trained implicitly like GANs via the private embedding and auxiliary information, where the learning is based on a stochastic procedure

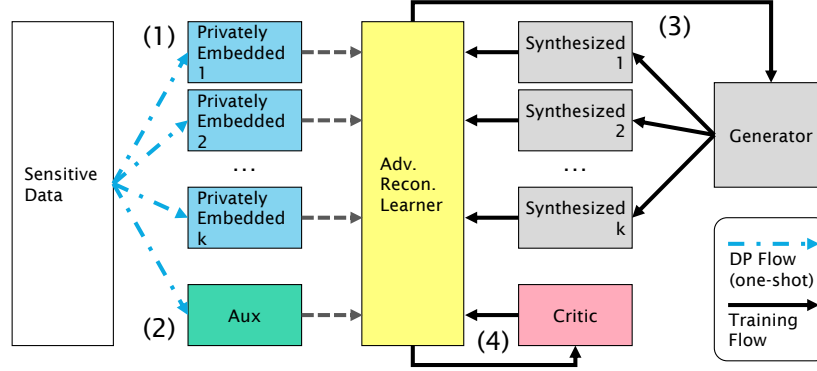


Figure 1: Overview of PEARL: (1) private embedding is obtained from the sensitive data, (2) auxiliary information is extracted privately, (3) a generator is trained with the private embedding and auxiliary information, (4) a critic is optimized to distinguish between the real and generated data.

that generates data, and (4) a critic distinguishing between the real and generated data. Note that unlike DP-SGD, there is no constraint on the number of training iteration or extensive tuning of clipping size in this framework. The overview of PEARL is illustrated in Fig. 1.

As a concrete realization of PEARL, We first identify that the characteristic function (CF) representation of data can be sanitized as the private embedding of PEARL. Consequently, it is possible to train deep generative models using an appropriately defined metric measuring the discrepancy between the real (but sanitized) and generated data distribution based on the CF without re-using the original data. As will be explained in detail in later Sections, the generative modelling approach using CFs also involves sampling “frequencies” from an *ad hoc* distribution, to project the data to the embedding. It is desirable to optimize the sampling distribution to better represent the data as an embedding, but the naive way of optimizing it would require re-accessing the data via sampling, coming at a cost of privacy budget. Henceforth, we also propose to incorporate a privacy-preserving critic to optimize the sampling strategy, which, through re-weighting, chooses the best representation from a fixed samples of frequencies without extra privacy costs.

To this end, we propose the following minimax optimization training objective:

$$\inf_{\theta \in \Theta} \sup_{\omega \in \Omega} \sum_{i=1}^k \frac{\omega(\mathbf{t}_i)}{\omega_0(\mathbf{t}_i)} |\tilde{\Phi}_{\mathbb{P}_r}(\mathbf{t}_i) - \hat{\Phi}_{\mathbb{Q}_\theta}(\mathbf{t}_i)|^2. \quad (1)$$

See later parts for notations and details. Theoretically, we show that our proposed objective has properties similar to those that are suited to training GANs, i.e., continuity and differentiability of the generator’s parameters, and continuity in weak topology. We also prove the consistency of our privacy-preserving sampling strategy at the asymptotic limit of infinite sampling. Empirical evaluations show that PEARL is able to high-quality synthetic data at reasonable privacy levels.

**Related work.** Recently, [18] has proposed DP-MERF, which first represents the sensitive data as random features in a DP manner and then learns a generator by minimizing the discrepancy between the (fixed) representation and generated data points. DP-MERF can iterate the learning process of the generator without further consuming the privacy budget; however, it is limited in the learning and generalization capabilities due to its fixed representation. Compared with our proposal, PEARL, DP-MERF may be viewed as a special case of ours, as PEARL improves the generator’s learning capability by incorporating characteristic function that makes adversarial training possible. Supplementary Sec. A provides a more detailed exposure to recent related works.

**Contributions.** Our contribution in this paper is three-fold: (i) We propose a general framework called PEARL, where, unlike DP-SGD, the generator training process and iteration is unconstrained, and ad-hoc hyperparameter tuning is not required. (ii) We demonstrate a realization of our framework by making use of the characteristic function and an adversarial re-weighting objective. (iii) Our proposal has theoretical guarantees of performance, and empirical evaluations show that our approach outperforms competitors at reasonable levels of privacy ( $\epsilon \simeq 1$ ).

**Organization.** The rest of the paper is organized as follows. We first provide preliminaries and background of the current work. Then, in Sec. 3, we describe the realization of PEARL and the generative modelling process. In Sec. 4, we continue the discussion of PEARL, focusing on the adversarial learning process. Theoretical guarantees of our proposal are also given. Experimental results are shown next in Sec. 5. Finally, we conclude.

**Ethics and social impacts.** This research advances the study of sharing data in a private manner using deep generative models. Differential privacy, recognized as a gold-standard concept for guaranteeing privacy, which is already being adopted in practice by the US Census Bureau for releasing census, is the core concept used in this research. Hence, it is potentially useful and applicable to other academic and industrial machine learning domains where sharing sensitive data without revealing personal information is important, thus bringing benefits to the machine learning community, as well as the society in general. That being said, differential privacy is still a relatively new technology, and must be handled with care, especially when setting the privacy budget, i.e., not adding enough noise to data might increase the risk of privacy violation.

## 2 Preliminaries

This Section gives a brief review of essential preliminaries about differential privacy, characteristic function and the related notations.

### 2.1 Differential Privacy

**Definition 1** ( $(\epsilon, \delta)$ -Differential Privacy). *Given privacy parameters  $\epsilon \geq 0$  and  $\delta \geq 0$ , a randomized mechanism,  $\mathcal{M} : \mathcal{D} \rightarrow \mathcal{R}$  with domain  $\mathcal{D}$  and range  $\mathcal{R}$  satisfies  $(\epsilon, \delta)$ -differential privacy (DP) if for any two adjacent inputs  $d, d' \in \mathcal{D}$  and for any subset of outputs  $S \subseteq \mathcal{R}$ , the following holds:*

$$\Pr[\mathcal{M}(d) \in S] \leq e^\epsilon \cdot \Pr[\mathcal{M}(d') \in S] + \delta. \quad (2)$$

We next consider concrete ways of sanitizing certain outputs with DP. A typical paradigm of DP is applying the randomized mechanism,  $\mathcal{M}$ , to a certain deterministic function  $f : \mathcal{D} \rightarrow \mathbb{R}$  such that the output of  $f$  is DP. The noise magnitude added by  $\mathcal{M}$  is determined by the *sensitivity* of  $f$ , defined as  $\Delta_f = \sup_{d, d' \in \mathcal{D}} \|f(d) - f(d')\|$ , where  $\|\cdot\|$  is a norm function defined on  $f$ 's output domain.  $d$  and  $d'$  are any adjacent pairs of dataset.

Laplacian and Gaussian mechanisms are the standard randomized mechanisms. We primarily utilize the Gaussian mechanism in this paper [13]:

**Definition 2** (Gaussian Mechanism). *Let  $f : X \rightarrow \mathbb{R}$  be an arbitrary function with sensitivity  $\Delta_f$ . The Gaussian Mechanism,  $\mathcal{M}_\sigma$ , parameterized by  $\sigma$ , adds noise to the output of  $f$  as follows:*

$$\mathcal{M}_\sigma(x) = f(x) + \mathcal{N}(0, \sigma^2 I). \quad (3)$$

One of the most important properties of DP relevant to our work is the post-processing theorem [13]. It ensures that the DP-sanitized data can be re-used without further consuming privacy budgets.

**Theorem 1** (Post-processing Theorem). *Let  $\mathcal{M} : \mathcal{D} \rightarrow \mathcal{R}$  be  $(\epsilon, \delta)$ -DP and let  $f : \mathcal{R} \rightarrow \mathcal{R}'$  be an arbitrary randomized function. Then,  $f \circ \mathcal{M} : \mathcal{D} \rightarrow \mathcal{R}'$  is  $(\epsilon, \delta)$ -DP.*

### 2.2 Characteristic Functions

Characteristic function (CF) is widely utilized in statistics and probability theory, and perhaps is best known to be used to prove the central limit theorem [44]. The definition is as follows.

**Definition 3** (Characteristic Function). *Given a random variable  $X \subseteq \mathbb{R}^d$  and  $\mathbb{P}$  as the probability measure associated with it, and  $\mathbf{t} \in \mathbb{R}^d$ , the corresponding characteristic function (CF) is given by*

$$\Phi_{\mathbb{P}}(\mathbf{t}) = \mathbb{E}_{\mathbf{x} \sim \mathbb{P}}[e^{i\mathbf{t} \cdot \mathbf{x}}] = \int_{\mathbb{R}^d} e^{i\mathbf{t} \cdot \mathbf{x}} d\mathbb{P}. \quad (4)$$

From the signal processing point of view, this mathematical operation is equivalent to the Fourier transformation, and  $\Phi_{\mathbb{P}}(\mathbf{t})$  is the Fourier transform at frequency  $\mathbf{t}$ . It is noted that we deal with the discrete approximation of CFs in practice. That is, given a dataset with  $n$  i.i.d. samples,  $\{\mathbf{x}_i\}_{i=1}^n$  from  $\mathbb{P}$ , the empirical CF is written as  $\hat{\Phi}_{\mathbb{P}}(\mathbf{t}) = \frac{1}{n} \sum_{i=1}^n e^{i\mathbf{t} \cdot \mathbf{x}_i}$ . We next introduce characteristic function distance (CFD) [20, 9]:

**Definition 4** (Characteristic Function Distance). *Given two distributions  $\mathbb{P}$  and  $\mathbb{Q}$  of random variables residing in  $\mathbb{R}^d$ , and  $\omega$  a sampling distribution on  $\mathbf{t} \in \mathbb{R}^d$ , the squared characteristic function distance (CFD) between  $\mathbb{P}$  and  $\mathbb{Q}$  is computed as:*

$$\mathcal{C}^2(\mathbb{P}, \mathbb{Q}) = \mathbb{E}_{\mathbf{t} \sim \omega(\mathbf{t})} [|\Phi_{\mathbb{P}}(\mathbf{t}) - \Phi_{\mathbb{Q}}(\mathbf{t})|^2] = \int_{\mathbb{R}^d} |\Phi_{\mathbb{P}}(\mathbf{t}) - \Phi_{\mathbb{Q}}(\mathbf{t})|^2 \omega(\mathbf{t}) d\mathbf{t}. \quad (5)$$

**Notations.** Let us make a short note on the notations before continuing. Let  $k$  be the number of  $\mathbf{t}$  drawn from  $\omega$  and  $\mathbb{P}$  be the probability measure of a random variable. We group the CFs associated to  $\mathbb{P}$  of different frequencies,  $(\hat{\Phi}_{\mathbb{P}}(\mathbf{t}_1), \dots, \hat{\Phi}_{\mathbb{P}}(\mathbf{t}_k))^{\top}$  more compactly as  $\hat{\phi}_{\mathbb{P}}(\mathbf{x})$ . To make the dependence of  $\hat{\phi}_{\mathbb{P}}(\mathbf{x})$  on the sampled data explicit, we also use the following notation:  $\hat{\phi}_{\mathbb{P}}(\mathbf{x}) = \frac{1}{n} \sum_{j=1}^n \hat{\phi}_{\mathbb{P}}(\mathbf{x}_j)$ . We also normalize  $\hat{\phi}_{\mathbb{P}}(\mathbf{x}_j)$  for any  $j$  such that  $\|\hat{\phi}_{\mathbb{P}}(\mathbf{x}_j)\|_2 = 1$ , where the norm is taken over the (complex) frequency space. With a slight abuse of notation, we abbreviate  $\hat{\phi}_{\mathbb{P}}$  as  $\hat{\phi}$  when there is no ambiguity in the underlying probability measure associated with the CF.

### 3 Generative Model of PEARL

Let us describe a realization of the PEARL framework. The first step in PEARL is projecting the sensitive data to an embedding before performing sanitization. We realize this by projecting the data to the CF as in Eq. 4, where the embedding's dimension is determined by the number of frequency drawn from the sampling distribution.

We choose to use CF as it has several attractive properties. CF is uniformly continuous and bounded, as can be seen from its expression in Eq. 4. Unlike the density function, the CF of a random variable always exists, and the uniqueness theorem implies that two distributions are identical if and only if the CFs of the random variables are equal [28].

#### 3.1 Private Embeddings with CFs

The CF is sanitized with DP by applying the Gaussian mechanism (Defn. 3) to  $\hat{\phi}(\mathbf{x})$ :

$$\tilde{\phi}(\mathbf{x}) = \hat{\phi}(\mathbf{x}) + \mathcal{N}(0, \Delta_{\hat{\phi}(\mathbf{x})}^2 \sigma^2 I), \quad (6)$$

where we write the sanitized CF as  $\tilde{\phi}(\mathbf{x})$ ;  $\Delta_{\hat{\phi}(\mathbf{x})}$  denotes the sensitivity of the CF,  $\sigma$  denotes the noise scale which is determined by the privacy budget,  $(\epsilon, \delta)$ .

Another reason we utilize the CF is that the calculation of sensitivity is tractable (no ad-hoc clipping *à la* DP-SGD), as shown below. Without loss of generality, consider two neighboring datasets of size  $n$  where only the last instance differs ( $\mathbf{x}_n \neq \mathbf{x}'_n$ ). The sensitivity of  $\hat{\phi}(\mathbf{x})$  may then be calculated as

$$\begin{aligned} \Delta_{\hat{\phi}(\mathbf{x})} &= \max_{\mathcal{D}, \mathcal{D}'} \left\| \frac{1}{n} \sum_{j=1}^n \hat{\phi}(\mathbf{x}_j) - \frac{1}{n} \sum_{j=1}^n \hat{\phi}(\mathbf{x}'_j) \right\|_2, \\ &= \max_{\mathbf{x}_n, \mathbf{x}'_n} \left\| \frac{1}{n} \hat{\phi}(\mathbf{x}_n) - \frac{1}{n} \hat{\phi}(\mathbf{x}'_n) \right\|_2 = \frac{2}{n}, \end{aligned}$$

where we have used triangle inequality and  $\|\hat{\phi}(\cdot)\|_2 = 1$ . Yet another advantage of using CFs is now apparent: the sensitivity is small as it is inversely proportional to the dataset size, which is important for controlling the magnitude of noise injection at practical privacy levels, as will be discussed in later Sections.

#### 3.2 Generative Modelling via CFs

Next, we would like to train a generative model where the CFs constructed from the generated data distribution,  $\mathcal{Y} \subseteq \mathbb{R}^d$ , matches those (sanitized) from the real data distribution,  $\mathcal{X} \subseteq \mathbb{R}^d$ .

A natural way of achieving this is via implicit generative modelling [29, 17]. We introduce a generative model parametrized by  $\theta$ ,  $G_{\theta} : \mathcal{Z} \rightarrow \mathbb{R}^d$ , which takes a low-dimensional latent vector  $z \in \mathcal{Z}$  sampled from a pre-determined distribution (e.g., Gaussian distribution) as the input.

In order to quantify the discrepancy between the real and generated data distribution, we use the CFD defined in Eq. 5. Empirically, when a finite number of frequencies,  $k$ , are sampled from  $\omega$ ,  $\mathcal{C}^2(\mathbb{P}, \mathbb{Q})$  is approximated by

$$\widehat{\mathcal{C}}^2(\mathbb{P}, \mathbb{Q}) = \frac{1}{k} \sum_{i=1}^k |\widehat{\Phi}_{\mathbb{P}}(\mathbf{t}_i) - \widehat{\Phi}_{\mathbb{Q}}(\mathbf{t}_i)|^2 \equiv \left\| \widehat{\Phi}_{\mathbb{P}}(\mathbf{x}) - \widehat{\Phi}_{\mathbb{Q}}(\mathbf{x}) \right\|_2^2, \quad (7)$$

where  $\widehat{\Phi}_{\mathbb{P}}(\mathbf{t})$  and  $\widehat{\Phi}_{\mathbb{Q}}(\mathbf{t})$  are the empirical CFs evaluated from i.i.d. samples of distributions  $\mathbb{P}$  and  $\mathbb{Q}$  respectively. Denoting the real data distribution by  $\mathbb{P}_r$ , and the output distribution of  $G_\theta$  by  $\mathbb{Q}_\theta$ , the training objective of the generator is to find the optimal  $\theta \in \Theta$  ( $\Theta$  being the space  $\theta$  lies in) that minimizes the empirical CFD:

$$\min_{\theta \in \Theta} \widehat{\mathcal{C}}^2(\mathbb{P}_r, \mathbb{Q}_\theta). \quad (8)$$

It can be shown via uniqueness theorem that as long as  $\omega$  resides in  $\mathbb{R}^d$ ,  $\mathcal{C}(\mathbb{P}, \mathbb{Q}) = 0 \iff \mathbb{P} = \mathbb{Q}$  [39]. This makes CFD an ideal distance metric for training the generator.

**Optimization procedure.** The generator parameter,  $\theta$ , is updated as follows.  $\widehat{\Phi}_{\mathbb{P}_r}(\mathbf{x})$  is first sanitized to obtain  $\widetilde{\Phi}_{\mathbb{P}_r}(\mathbf{x})$ , as in Eq. 6. This is performed only for once (one-shot). Then, at each iteration,  $m$  samples of  $\mathbf{z}$  are drawn to calculate  $\widehat{\Phi}_{\mathbb{Q}_\theta}(\mathbf{x})$ . Gradient updates on  $\theta$  are performed by minimizing the CFD,  $\left\| \widetilde{\Phi}_{\mathbb{P}_r}(\mathbf{x}) - \widehat{\Phi}_{\mathbb{Q}_\theta}(\mathbf{x}) \right\|_2$ .

We note that only the first term,  $\widetilde{\Phi}(\mathbf{x})$ , has access to the real data distribution,  $\mathcal{X}$ , of which privacy is of concern. Then, by Thm. 1,  $G_\theta$  trained with respect to  $\widetilde{\Phi}(\mathbf{x})$  is DP. Furthermore, unlike DP-SGD, the training of  $G_\theta$  is not limited by network size/layers or training iterations. Once the sanitized CF is released, there is no additional constraints due to privacy on the training procedure. We summarize the above results in the following proposition:

**Proposition 1.** *The generator  $G_\theta$  trained to optimize Eq. 8 with  $\widetilde{\Phi}(\mathbf{x})$  sanitized according to Eq. 6 satisfies  $(\epsilon, \delta)$ -DP, where  $\sigma \geq \sqrt{2 \log(1.25/\delta)}/\epsilon$ .*

### 3.3 Improving Generative Modelling

We propose several variants of PEARL that help improve the generative modelling ability.

**Conditional CFs.** We first introduce the conditional version of CF. The main usage of conditional CFs is to generate data conditioned on class labels  $y$ . As  $p(x) = \int p(x|y)p(y)dy$ , the empirical CF conditioned on  $y$  is rewritten as follows:

$$\widehat{\Phi}(\mathbf{x}, y_i) = \frac{1}{m} \sum_{j=1}^m \sum_{i=1}^{Y_i} \widehat{\Phi}(\mathbf{x}_j, y_i), \quad \widehat{\Phi}(\mathbf{x}) = \sum_{y=1}^Y \widehat{\Phi}(\mathbf{x}, y) \quad (9)$$

where  $Y_i$  is the total number of data instances conditioned on  $y = y_i$ , and  $Y$  is the total number of labels. Similar to conditional GAN [31], the generator is fed with a concatenated input of the noise  $z$  and  $y$ , i.e.,  $G_\theta(\mathcal{Z}, \mathcal{Y})$ . Then, Eq. 7 may be rewritten as

$$\widehat{\mathcal{C}}^2(\mathbb{P}_r, \mathbb{Q}_\theta) = \frac{1}{k} \sum_{i=1}^k \sum_{j=1}^Y |\widehat{\Phi}_{\mathbb{P}_r}(\mathbf{t}_i, y_j) - \widehat{\Phi}_{\mathbb{Q}_\theta}(\mathbf{t}_i, y_j)|^2. \quad (10)$$

The sensitivity for the conditional case remains the same as those presented in Sec. 3.1:  $\Delta_{\widehat{\Phi}_i(\mathbf{x}, y)} = 2/m$ , where we have made the dependence on the condition  $y$  explicit. The Gaussian mechanism may then be used to sanitize the conditional CF in order to achieve DP.

**DP release of auxiliary information.** Auxiliary information regarding to the dataset useful for generating data with better quality may be released under DP. The total privacy budget due to multiple releases of information is accounted for using the Rényi DP composition.<sup>1</sup> Several examples of auxiliary information are given in Supplementary Sec. E.

<sup>1</sup>We use the *autodp* package to keep track of the privacy budget [43]. See Supplementary Sec. B for the definition of Rényi DP.

## 4 Adversarial Reconstruction Learning

This Section is devoted to proposing a privacy-preserving critic for optimizing  $\omega(\mathbf{t})$ , while giving provable guarantees of performance.

### 4.1 Distribution Optimization

Back to Eq. 5 and Eq. 7, we note that choosing a “good”  $\omega(\mathbf{t})$  or a “good” set of sampled frequencies is vital at helping to discriminate between  $\mathbb{P}$  and  $\mathbb{Q}$ . For example, if the difference between  $\mathbb{P}$  and  $\mathbb{Q}$  lies in the high-frequency region, one should choose to use  $\mathbf{t}$  with large values to, in the language of two-sample testing, improve the test power.

**Adversarial objective.** If the resulting empirical CFD remains small due to under-optimized  $\omega(\mathbf{t})$ , while the two distributions still differ significantly, the generator cannot be optimally trained to generate high-quality samples resembling the real data. Hence, we consider training the generator by, in addition to minimizing the empirical CFD, maximizing the empirical CFD using an *adversarial objective* which acts as a *critic*, where the empirical CFD is maximized by finding the best sampling distribution. We consider a training objective of the form

$$\inf_{\theta \in \Theta} \sup_{\omega \in \Omega} \widehat{\mathcal{C}}_{\omega}^2(\mathbb{P}_r, \mathbb{Q}_{\theta}), \quad (11)$$

where  $\Omega$  is some set of probability distribution space of which the sampling distribution  $\omega$  lives in.

**Privacy-preserving optimization.** It is intractable to directly optimize  $\omega$  in the integral form as in Eq. 5. A conventional way of resolving this is to use the reparametrization trick [23]. This involves sampling  $\mathbf{t}$  from a pre-determined distribution, and transform it via a deterministic function  $\omega = h_{\psi}(\mathbf{t})$  parametrized by  $\psi$ , where optimizing  $\omega$  is reparametrized as optimizing  $\psi$  via gradient backpropagation. However, such a procedure is *not privacy-preserving*. This is because it involves re-calculating the data-dependent  $\tilde{\phi}(\mathbf{x})$  using updated  $\mathbf{t}$ , leading to privacy degradation at each iteration. In this work, we instead opt for a *one-shot* sampling strategy where once the private data is released, no additional privacy-induced constraints on training procedures are incurred. We believe that such a new formulation of distribution learning alternative to the reparametrization trick is of independent interest as well.

Recall from Sec. 3 that the empirical CFD,  $\widehat{\mathcal{C}}^2(\mathbb{P}_r, \mathbb{Q}_{\theta}) = \frac{1}{k} \sum_{i=1}^k |\tilde{\Phi}_{\mathbb{P}_r}(\mathbf{t}_i) - \hat{\Phi}_{\mathbb{Q}_{\theta}}(\mathbf{t}_i)|^2$ , is obtained by drawing  $k$  frequencies from a base distribution  $\omega_0$ . Our idea is to find a (weighted) set of frequencies that gives the best test power from the drawn set. We propose Eq. 1 as the optimization objective, restated below:

$$\inf_{\theta \in \Theta} \sup_{\omega \in \Omega} \sum_{i=1}^k \frac{\omega(\mathbf{t}_i)}{\omega_0(\mathbf{t}_i)} |\tilde{\Phi}_{\mathbb{P}_r}(\mathbf{t}_i) - \hat{\Phi}_{\mathbb{Q}_{\theta}}(\mathbf{t}_i)|^2.$$

Note that the generator trained with this objective still satisfies DP as given in Prop. 1 due to Thm. 1. The following Lemma ensures that the discrete approximation of the inner maximization of Eq. 1 approaches the population optimum as the number of sampling frequency increases ( $k \rightarrow \infty$ ):

**Lemma 1.** *Let  $\omega_0$  be any probability distribution defined on  $\mathcal{R}^d$ , and let  $f : \mathcal{R}^d \rightarrow \mathcal{R}'$  be any function. Also let  $\mathbf{t} \in \mathcal{R}^d$  and  $\omega^*$  be the maximal distribution of  $\omega$  with respect to  $\mathbb{E}_{\omega}[f(\mathbf{t})] \equiv \int f(\mathbf{t})\omega(\mathbf{t})d\mathbf{t}$ . Assume that the empirical approximation  $\hat{\mathbb{E}}_{\omega}[f(\mathbf{t})] \rightarrow \mathbb{E}_{\omega}[f(\mathbf{t})]$  at the asymptotic limit for any  $\omega$ . Then,  $\hat{\mathbb{E}}_{\omega_0}[f(\mathbf{t})\frac{\omega^*(\mathbf{t})}{\omega_0(\mathbf{t})}] \rightarrow \mathbb{E}_{\omega^*}[f(\mathbf{t})]$  at the asymptotic limit as well.*

The proof is in Supplementary Sec. C, and is based on importance sampling. Empirically, we find that treating  $\omega(\mathbf{t}_i)$  as a free parameter and optimizing it directly does not lead to improvement in performance. This may be due to the optimization procedure focusing too much on uninformative frequencies that contain merely noises due to DP or sampling. We perform *parametric* optimization instead, that is, e.g., we perform optimization with respect to  $\{\boldsymbol{\mu}, \boldsymbol{\sigma}\}$  if  $\omega$  is of the Gaussian form,  $\mathcal{N}(\boldsymbol{\mu}, \boldsymbol{\sigma}^2)$ .

### 4.2 Further Analyses

**Effectiveness of the critic.** To further motivate why it is preferable to introduce an adversarial objective as in Eq. 11, we present a simple demonstration through the lens of two-sample

testing [9, 22] using synthetic data generated from Gaussian distributions. We generate two unit-variance multivariate Gaussian distributions  $\mathbb{P}, \mathbb{Q}$ , where all dimensions but one have zero mean ( $\mathbb{P} \sim \mathcal{N}(\mathbf{0}_d, \mathbf{I}_d)$ ,  $\mathbb{Q} \sim \mathcal{N}((1, 0, \dots, 0)^\top, \mathbf{I}_d)$ ). We conduct a two-sample test using the CF to distinguish between the two distributions, which gets more difficult as the dimensionality increases. We test if the null hypothesis where the samples are drawn from the same distribution is rejected. Higher rejection rate indicates better test power.

Note that the first dimension (where the distribution differs) of the frequency used to construct CFs is the most discriminative dimension for distinguishing the distributions. We first consider an “unoptimized” set of frequencies of size 20, where only one of them is discriminative. A “normal” set of frequencies is also considered for comparison, where the frequencies are sampled randomly from a multivariate Gaussian distributions. Finally, we consider an “optimized” set of frequencies, where we re-weight the set of unoptimized frequencies such that only the discriminative one has non-zero weight. More details can be found in Supplementary Sec. D.

Fig. 2 shows the hypothesis rejection rate versus the number of dimensions for the three cases considered above. As can be observed from the Figure, the “optimized” case gives overall the best test power. While this experiment is somewhat contrived, it can be understood that although both “unoptimized” and “optimized” sets of frequencies contain the discriminative  $\mathbf{t}_0$ , the re-weighting procedure of selecting the most discriminative CF improves the test power significantly. Even without re-sampling from a “better”  $\omega(\mathbf{t})$ , re-weighting the existing frequencies can improve the test power. The fact that re-weighting can improve the test power is crucial privacy-wise because the alternative method, re-sampling, causes degradation in privacy.

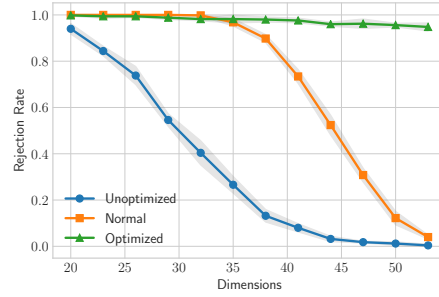


Figure 2: Increased test power upon optimization (green) in two-sample test.

**Performance guarantees.** Let us discuss the theoretical properties of Eq. 11. The objective defined in Eq. 11 shares beneficial properties similar to those required to train good GANs, first formulated in the Wasserstein GAN paper [3]. First, the generator learns from a distance continuous and differentiable almost everywhere within the generator’s parameters. Second, the distance is continuous in weak topology, and thus provides informative feedback to the generator (different from, e.g., the Jensen-Shannon divergence, which does not satisfy this property).

We make assumptions similar to those given in [3], and state the first theorem as follows.

**Theorem 2.** *Assume that  $G_\theta(z)$  is locally Lipschitz with respect to  $(\theta, z)$ ; there exists  $L((\theta, z))$  satisfying  $\mathbb{E}_z [L(\theta, z)] < \infty$ ; and  $\sup_{\omega \in \Omega} \mathbb{E}_\omega [\|\mathbf{t}\|] < \infty$  for all  $\mathbf{t}$ . Then, the function  $\sup_{\omega \in \Omega} \mathcal{C}_\omega^2(\mathbb{P}_r, \mathbb{Q}_\theta)$  is continuous in  $\theta \in \Theta$  everywhere, and differentiable in  $\theta \in \Theta$  almost everywhere.*

Note that the local Lipschitz assumptions are satisfied by commonly used neural network components, such as fully connected layers and ReLU activations. The continuity and differentiability conditions with respect to  $\theta$  stated above allow  $G_\theta$  to be trained via gradient descent. The theorem related to continuity in weak topology is the following:

**Theorem 3.** *Let  $\mathbb{P}$  be a distribution on  $\mathcal{X}$  and  $(\mathbb{P}_n)_{n \in \mathbb{N}}$  be a sequence of distributions on  $\mathcal{X}$ . Under the assumption  $\sup_{\omega \in \Omega} \mathbb{E}_{\omega(\mathbf{t})} [\|\mathbf{t}\|] < \infty$ , the function  $\sup_{\omega \in \Omega} \mathcal{C}_\omega^2(\mathbb{P}_n, \mathbb{P})$  is continuous in the weak topology, i.e., if  $\mathbb{P}_n \xrightarrow{D} \mathbb{P}$ , then  $\sup_{\omega \in \Omega} \mathcal{C}_\omega^2(\mathbb{P}_n, \mathbb{P}) \xrightarrow{D} 0$ , where  $\xrightarrow{D}$  denotes convergence in distribution.*

Weakness is desirable as the easier (weaker) it is for the distributions to converge, the easier it will be for the model to learn to fit the data distribution. The core ideas used to prove both of these theorems are the fact that the difference of the CFs (which is of the form  $e^{ia}$ ) can be bounded as follows:  $|e^{ia} - e^{ib}| \leq |a - b|$ , and showing that the function is locally Lipschitz, which ensures the desired properties of continuity and differentiability. See Supplementary Sec. C for the full proofs.

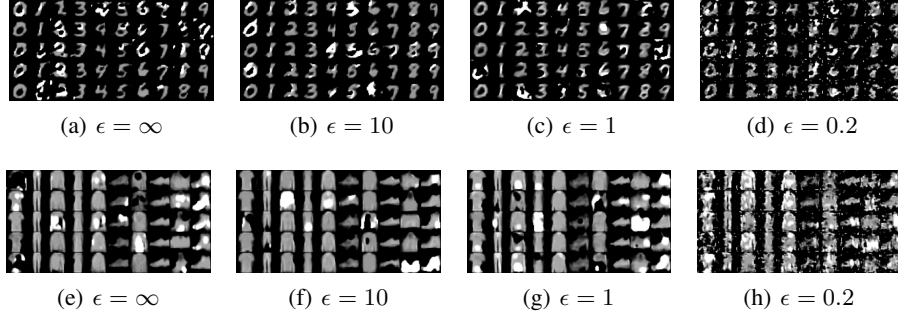


Figure 3: Generated MNIST and Fashion-MNIST samples for various values of  $\epsilon$  and  $\delta = 10^{-5}$ .

## 5 Experiments

### 5.1 Experimental Setup

To test the efficacy of PEARL, we perform empirical evaluations on three datasets, namely MNIST [25], Fashion-MNIST [45] and Adult [10].<sup>2</sup> Neural networks constructed from convolutional and fully connected layers are utilized as the generator for image and tabular datasets respectively. Detailed setups are available in Supplementary Sec. I.

**Training Procedure.** As our training involves minimax optimization (Eq. 1), we perform gradient descent updates based on the minimization and maximization objectives alternately. We use a zero-mean diagonal standard-deviation Gaussian distribution,  $\mathcal{N}(\mathbf{0}, \text{diag}(\sigma^2))$  as the sampling distribution,  $\omega$ . Maximization is performed with respect to  $\sigma$ . The pseudo-code of the full algorithm is presented in Supplementary Sec. G.

**Evaluation Metrics.** In the main text and Supplementary Sec. J, we show qualitative results, i.e., synthetic images (image dataset) and histograms (tabular dataset) generated with PEARL. Furthermore, for image datasets, the Fréchet Inception Distance (FID) [21] and Kernel Inception Distance (KID) [6] are used to evaluate the quantitative performance. For tabular data, we use the synthetic data as the training data of 10 scikit-learn classifiers [37] and evaluate the classifiers' performances on real test data. ROC (area under the receiver operating characteristics curve) and PRC (area under the precision recall curve) are the evaluation metrics. We provide the definitions and details of FID and KID in Supplementary Sec. H.

### 5.2 Evaluation Details

**MNIST and Fashion-MNIST.** During training, we fix the inverse standard deviation of the base distribution,  $\omega_0$ , to be the DP estimate of the mean of the pairwise distance of the data, motivated by the median heuristic [16]. Mean is estimated instead of median as its sensitivity is more tractable when considering neighboring datasets. See Supplementary Sec. F for the calculation of the DP estimate. Privacy budget is allocated equally between the sanitization of CFs and the release of auxiliary information.

Some of the generated images are shown in Fig. 3. At the non-private limit ( $\epsilon = \infty$ ), the quality of the images is worse than other popular non-private approaches such as GANs. This is due to two reasons. First, the original data is projected to a lower dimension, losing some information in the process. Second, our architecture does not have a discriminator-like network as in the vanilla GAN framework to improve the generative modelling capability. However, we notice that the quality of the images does not drop much as the privacy level increases (except at  $\epsilon = 0.2$ , where the quality starts to degrade visibly). This can be understood from arguments given below Eq. 6, where it is shown that the noise added to the CFs is small as it scales inversely proportional to the total sample size. It also indicates that our approach works particularly well at practical levels of privacy. We now provide quantitative results by performing evaluation at  $(\epsilon, \delta) = (1, 10^{-5})$ . We compare PEARL

<sup>2</sup>Source codes for running our experiments will be available upon publication.



Datasets	Metrics	DP-MERF	Ours (Min only)	Ours (Minimax)
MNIST	FID	$49.9 \pm 0.22$	$3.79 \pm 0.06$	<b><math>3.52 \pm 0.06</math></b>
	KID ( $\times 10^3$ )	$148 \pm 46.2$	$77.8 \pm 9.88$	<b><math>70.5 \pm 10.3</math></b>
Fashion-MNIST	FID	$37.0 \pm 0.15$	$1.99 \pm 0.04$	<b><math>1.92 \pm 0.04</math></b>
	KID ( $\times 10^3$ )	$1220 \pm 36.1$	<b><math>24.0 \pm 6.90</math></b>	$26.9 \pm 6.80$

Table 1: FID and KID (lower is better) on image datasets at  $(\epsilon, \delta) = (1, 10^{-5})$ .

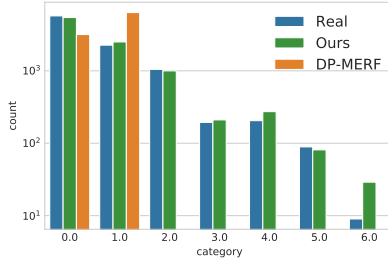


Figure 4: Plot of histogram for the “marital-status” attribute of the Adult dataset. Evaluation is performed at  $(\epsilon, \delta) = (1, 10^{-5})$ .

Data	Metrics	Average
Real data	ROC	$0.765 \pm 0.047$
	PRC	$0.654 \pm 0.050$
DP-MERF	ROC	$0.641 \pm 0.044$
	PRC	$0.536 \pm 0.034$
Ours	ROC	<b><math>0.721 \pm 0.035</math></b>
	PRC	<b><math>0.618 \pm 0.033</math></b>

Table 2: Average ROC and PRC scores for the Adult dataset evaluated at  $(\epsilon, \delta) = (1, 10^{-5})$ .

mainly with DP-MERF [18], as other methods do not produce usable images at single-digit  $\epsilon$ .<sup>3</sup> We run the experiment five times (with different random seeds each time), and for each time, 60k samples are generated to evaluate the FID and KID. In Table 1, the FID and KID (average and error) of DP-MERF, PEARL but without maximization, and PEARL (with maximization) are shown. It can be seen that PEARL outperforms DP-MERF significantly, and the maximization procedure leads to improvement in the scores.

**Adult.** The Adult dataset consists of continuous and categorical features. As data pre-processing, continuous features are scaled to  $[0, 1]$ ,<sup>4</sup> while categorical features are one-hot encoded. We also compare our results with DP-MERF, as DP-MERF performs best among other existing methods. As in DP-MERF, to deal with class imbalance, auxiliary information of class counts are released with DP to re-weight the CF of each class. Again, auxiliary information and CFs share equal budget of privacy, and we perform evaluation at  $(\epsilon, \delta) = (1, 10^{-5})$ . 11k synthetic samples are generated for evaluation.

A plot of histogram of the “marital-status” attribute comparing the real and synthetic data is shown in Fig. 4. As can be observed in the Figure, PEARL is able to model the real data better than DP-MERF, covering more modes in the categorical variable with less discrepancy in the frequency of each mode. The average ROC and PRC scores (average and error) are shown in Table 2. ROC and PRC scores based on PEARL’s training data are shown to be closer to those based on real training data compared to DP-MERF. In Supplementary Sec. J, we show more detailed results, including more histogram plots, and the scores of each classifier. Overall, we have demonstrated that PEARL is able to produce high-quality synthetic data at practical privacy levels.

## 6 Conclusion

We have developed a DP framework to synthesize data with deep generative models. Our approach provides synthetic samples at practical privacy levels, and sidesteps difficulties encountered in DP-SGD. We comment on several potential future directions. While we have limited ourselves to characteristic functions, it is interesting to adopt and adapt other GAN paradigms to the PEARL framework (e.g., IPM-GANs which are discussed in Supplementary Sec. A). Moreover, throughout the current work, we have taken the extreme limit where the sensitive data is transformed, sanitized, and released in a one-shot fashion. Allowing more accesses to the data could be more beneficial in terms of the privacy-utility trade-off. We intend to study these aspects in the future.

<sup>3</sup>As DP-MERF also uses a sampling distribution but does not allocate privacy budget for calculating the parameters of the sampling distribution, we fix its sampling distribution to be  $\mathcal{N}(\mathbf{0}, \text{diag}(\mathbf{1}))$ .

<sup>4</sup>For visualization, we map the results back to the original domain.

## References

- [1] Martin Abadi, Andy Chu, Ian Goodfellow, H Brendan McMahan, Ilya Mironov, Kunal Talwar, and Li Zhang. Deep learning with differential privacy. In *Proceedings of the 2016 ACM SIGSAC Conference on Computer and Communications Security*, pages 308–318. ACM, 2016.
- [2] Abdul Fatir Ansari, Jonathan Scarlett, and Harold Soh. A characteristic function approach to deep implicit generative modeling. In *IEEE Conference on Computer Vision and Pattern Recognition*, 2020.
- [3] Martín Arjovsky, Soumith Chintala, and Léon Bottou. Wasserstein gan. *ArXiv*, abs/1701.07875, 2017.
- [4] Eugene Bagdasaryan, Omid Poursaeed, and Vitaly Shmatikov. Differential privacy has disparate impact on model accuracy. In Hanna M. Wallach, Hugo Larochelle, Alina Beygelzimer, Florence d’Alché-Buc, Emily B. Fox, and Roman Garnett, editors, *Advances in Neural Information Processing Systems 32: Annual Conference on Neural Information Processing Systems 2019, NeurIPS 2019, December 8-14, 2019, Vancouver, BC, Canada*, pages 15453–15462, 2019.
- [5] Marc G Bellemare, Ivo Danihelka, Will Dabney, Shakir Mohamed, Balaji Lakshminarayanan, Stephan Hoyer, and Rémi Munos. The Cramer distance as a solution to biased Wasserstein gradients. *arXiv preprint arXiv:1705.10743*, 2017.
- [6] Mikołaj Bińkowski, Dougal J Sutherland, Michael Arbel, and Arthur Gretton. Demystifying MMD GANs. *arXiv preprint arXiv:1801.01401*, 2018.
- [7] Dingfan Chen, Tribhuvanesh Orekondy, and Mario Fritz. Gs-wgan: A gradient-sanitized approach for learning differentially private generators. In *Advances in Neural Information Processing Systems 33*, 2020.
- [8] Rui Chen, Qian Xiao, Yu Zhang, and Jianliang Xu. Differentially private high-dimensional data publication via sampling-based inference. In *Proceedings of the 21th ACM SIGKDD International Conference on Knowledge Discovery and Data Mining*, pages 129–138, 2015.
- [9] Kacper P Chwialkowski, Aaditya Ramdas, Dino Sejdinovic, and Arthur Gretton. Fast two-sample testing with analytic representations of probability measures. In *Advances in Neural Information Processing Systems*, pages 1981–1989, 2015.
- [10] Dheeru Dua and Casey Graff. UCI machine learning repository, 2017.
- [11] Cynthia Dwork. Differential privacy. In *Proceedings of the 33rd international conference on Automata, Languages and Programming-Volume Part II*, pages 1–12. Springer-Verlag, 2006.
- [12] Cynthia Dwork. A firm foundation for private data analysis. *Communications of the ACM*, 54(1):86–95, 2011.
- [13] Cynthia Dwork and Aaron Roth. The algorithmic foundations of differential privacy. *Found. Trends Theor. Comput. Sci.*, 9:211–407, August 2014.
- [14] Herbert Federer. *Geometric measure theory*. Springer, 2014.
- [15] Lorenzo Frigerio, Anderson Santana de Oliveira, Laurent Gomez, and Patrick Duverger. Differentially private generative adversarial networks for time series, continuous, and discrete open data. In *ICT Systems Security and Privacy Protection - 34th IFIP TC 11 International Conference, SEC 2019, Lisbon, Portugal, June 25-27, 2019, Proceedings*, pages 151–164, 2019.
- [16] Damien Garreau, Wittawat Jitkrittum, and Motonobu Kanagawa. Large sample analysis of the median heuristic, 2018.
- [17] Ian Goodfellow, Jean Pouget-Abadie, Mehdi Mirza, Bing Xu, David Warde-Farley, Sherjil Ozair, Aaron Courville, and Yoshua Bengio. Generative adversarial nets. In *Advances in Neural Information Processing Systems*, pages 2672–2680, 2014.

- [18] Frederik Harder, Kamil Adamczewski, and Mijung Park. DP-MERF: differentially private mean embeddings with random features for practical privacy-preserving data generation. In Arindam Banerjee and Kenji Fukumizu, editors, *The 24th International Conference on Artificial Intelligence and Statistics, AISTATS 2021, April 13-15, 2021, Virtual Event*, volume 130 of *Proceedings of Machine Learning Research*, pages 1819–1827. PMLR, 2021.
- [19] Moritz Hardt, Katrina Ligett, and Frank Mcsherry. A simple and practical algorithm for differentially private data release. In F. Pereira, C. J. C. Burges, L. Bottou, and K. Q. Weinberger, editors, *Advances in Neural Information Processing Systems 25*, pages 2339–2347. Curran Associates, Inc., 2012.
- [20] CE Heathcote. A test of goodness of fit for symmetric random variables. *Australian Journal of Statistics*, 14(2):172–181, 1972.
- [21] Martin Heusel, Hubert Ramsauer, Thomas Unterthiner, Bernhard Nessler, and Sepp Hochreiter. GANs trained by a two time-scale update rule converge to a local Nash equilibrium. In *Advances in Neural Information Processing Systems*, pages 6626–6637, 2017.
- [22] Wittawat Jitkrittum, Zoltán Szabó, Kacper P. Chwialkowski, and Arthur Gretton. Interpretable distribution features with maximum testing power. In Daniel D. Lee, Masashi Sugiyama, Ulrike von Luxburg, Isabelle Guyon, and Roman Garnett, editors, *Advances in Neural Information Processing Systems 29: Annual Conference on Neural Information Processing Systems 2016, December 5-10, 2016, Barcelona, Spain*, pages 181–189, 2016.
- [23] Diederik P Kingma and Max Welling. Auto-encoding variational bayes. *arXiv preprint arXiv:1312.6114*, 2013.
- [24] Achim Klenke. *Probability theory: a comprehensive course*. Springer Science & Business Media, 2013.
- [25] Yann LeCun, Corinna Cortes, and CJ Burges. Mnist handwritten digit database. *ATT Labs [Online]*. Available: <http://yann.lecun.com/exdb/mnist>, 2, 2010.
- [26] Chun-Liang Li, Wei-Cheng Chang, Yu Cheng, Yiming Yang, and Barnabás Póczos. MMD gan: Towards deeper understanding of moment matching network. In *Advances in Neural Information Processing Systems*, pages 2203–2213, 2017.
- [27] Shengxi Li, Zeyang Yu, Min Xiang, and Danilo P. Mandic. Reciprocal adversarial learning via characteristic functions. In Hugo Larochelle, Marc’Aurelio Ranzato, Raia Hadsell, Maria-Florina Balcan, and Hsuan-Tien Lin, editors, *Advances in Neural Information Processing Systems 33: Annual Conference on Neural Information Processing Systems 2020, NeurIPS 2020, December 6-12, 2020, virtual*, 2020.
- [28] Eugene Lukacs. A survey of the theory of characteristic functions. *Advances in Applied Probability*, 4(1):1–37, 1972.
- [29] David J.C MacKay. Bayesian neural networks and density networks. *Nuclear Instruments and Methods in Physics Research Section A: Accelerators, Spectrometers, Detectors and Associated Equipment*, 354(1):73–80, 1995. Proceedings of the Third Workshop on Neutron Scattering Data Analysis.
- [30] Ilya Mironov. Rényi differential privacy. In *2017 IEEE 30th Computer Security Foundations Symposium (CSF)*, pages 263–275. IEEE, 2017.
- [31] Mehdi Mirza and Simon Osindero. Conditional generative adversarial nets. *CoRR*, abs/1411.1784, 2014.
- [32] Noman Mohammed, Rui Chen, Benjamin C.M. Fung, and Philip S. Yu. Differentially private data release for data mining. In *Proceedings of the 17th ACM SIGKDD International Conference on Knowledge Discovery and Data Mining, KDD ’11*, pages 493–501, New York, NY, USA, 2011. ACM.
- [33] Youssef Mroueh and Tom Sercu. Fisher GAN. In *Advances in Neural Information Processing Systems*, pages 2513–2523, 2017.

- [34] Youssef Mroueh, Tom Sercu, and Vaibhava Goel. McGAN: Mean and covariance feature matching gan. *arXiv preprint arXiv:1702.08398*, 2017.
- [35] Nicolas Papernot, Martín Abadi, Úlfar Erlingsson, Ian Goodfellow, and Kunal Talwar. Semi-supervised Knowledge Transfer for Deep Learning from Private Training Data. In *Proceedings of the International Conference on Learning Representations (ICLR)*, April 2017.
- [36] Mijung Park, James R. Foulds, Kamalika Choudhary, and Max Welling. DP-EM: differentially private expectation maximization. In Aarti Singh and Xiaojin (Jerry) Zhu, editors, *Proceedings of the 20th International Conference on Artificial Intelligence and Statistics, AISTATS 2017, 20-22 April 2017, Fort Lauderdale, FL, USA*, volume 54 of *Proceedings of Machine Learning Research*, pages 896–904. PMLR, 2017.
- [37] F. Pedregosa, G. Varoquaux, A. Gramfort, V. Michel, B. Thirion, O. Grisel, M. Blondel, P. Prettenhofer, R. Weiss, V. Dubourg, J. Vanderplas, A. Passos, D. Cournapeau, M. Brucher, M. Perrot, and E. Duchesnay. Scikit-learn: Machine learning in Python. *Journal of Machine Learning Research*, 12:2825–2830, 2011.
- [38] Wahbeh Qardaji, Weining Yang, and Ninghui Li. Privview: practical differentially private release of marginal contingency tables. In *Proceedings of the 2014 ACM SIGMOD international conference on Management of data*, pages 1435–1446, 2014.
- [39] Bharath K Sriperumbudur, Kenji Fukumizu, and Gert RG Lanckriet. Universality, characteristic kernels and rkhs embedding of measures. *Journal of Machine Learning Research*, 12(7), 2011.
- [40] Shun Takagi, Tsubasa Takahashi, Yang Cao, and Masatoshi Yoshikawa. P3GM: private high-dimensional data release via privacy preserving phased generative model. *CoRR*, abs/2006.12101, 2020.
- [41] Tsubasa Takahashi, Shun Takagi, Hajime Ono, and Tatsuya Komatsu. Differentially private variational autoencoders with term-wise gradient aggregation. *CoRR*, abs/2006.11204, 2020.
- [42] Reihaneh Torkzadehmahani, Peter Kairouz, and Benedict Paten. Dp-cgan: Differentially private synthetic data and label generation. In *The IEEE Conference on Computer Vision and Pattern Recognition (CVPR) Workshops*, June 2019.
- [43] Yu-Xiang Wang, Borja Balle, and Shiva Prasad Kasiviswanathan. Subsampled renyi differential privacy and analytical moments accountant. In Kamalika Chaudhuri and Masashi Sugiyama, editors, *Proceedings of Machine Learning Research*, volume 89 of *Proceedings of Machine Learning Research*, pages 1226–1235. PMLR, April 2019.
- [44] David Williams. *Probability with martingales*. Cambridge University Press, 1991.
- [45] Han Xiao, Kashif Rasul, and Roland Vollgraf. Fashion-mnist: a novel image dataset for benchmarking machine learning algorithms. *arXiv preprint arXiv:1708.07747*, 2017.
- [46] Yonghui Xiao, Li Xiong, and Chun Yuan. Differentially private data release through multidimensional partitioning. In Willem Jonker and Milan Petković, editors, *Secure Data Management*, pages 150–168, Berlin, Heidelberg, 2010. Springer Berlin Heidelberg.
- [47] Liyang Xie, Kaixiang Lin, Shu Wang, Fei Wang, and Jiayu Zhou. Differentially private generative adversarial network. *CoRR*, abs/1802.06739, 2018.
- [48] Lei Xu, Maria Skoularidou, Alfredo Cuesta-Infante, and Kalyan Veeramachaneni. Modeling tabular data using conditional gan. In H. Wallach, H. Larochelle, A. Beygelzimer, F. d'Alché-Buc, E. Fox, and R. Garnett, editors, *Advances in Neural Information Processing Systems*, volume 32. Curran Associates, Inc., 2019.
- [49] Jinsung Yoon, James Jordon, and Mihaela van der Schaar. PATE-GAN: Generating synthetic data with differential privacy guarantees. In *International Conference on Learning Representations*, 2019.
- [50] Jun Zhang, Graham Cormode, Cecilia M Procopiuc, Divesh Srivastava, and Xiaokui Xiao. Privbayes: Private data release via bayesian networks. *ACM Transactions on Database Systems (TODS)*, 42(4):1–41, 2017.

- [51] T. Zhu, G. Li, W. Zhou, and P. S. Yu. Differentially private data publishing and analysis: A survey. *IEEE Transactions on Knowledge and Data Engineering*, 29(8):1619–1638, August 2017.

# Supplementary Material

## A Related Works

**IPM-GANs.** Our approach is partially inspired by our observations in a class of GANs which is based on the integral probability metric (IPM). Generally speaking, the training objective of the IPM-GAN generator is minimizing a distance metric measuring the difference between the data distribution ( $\mathbb{P}_r$ ) and generated data distribution ( $\mathbb{Q}_\theta$ ) which has the following form:

$$d(\mathbb{P}_r, \mathbb{Q}_\theta) = \sup_{f \in \mathcal{F}} |\mathbb{E}_{x \sim \mathbb{P}_r}[f(x)] - \mathbb{E}_{x \sim \mathbb{Q}_\theta}[f(x)]|, \quad (12)$$

where  $\mathcal{F}$  is a set of bounded functions acting as a *critic* telling apart synthetic samples from real samples. Wasserstein GAN [3], Cramer GAN [5], McGAN [34], Fisher GAN [33], and MMD-GAN [26, 6] are some of the variations of IPM-GANs found in the literature. More recently, IPM-GANs utilizing CFs have also been explored [2, 27].

One distinctive difference of our approach compared to IPM-GANs is the lack of a critic that interacts with data directly in our architecture. This is because training a critic in the IPM-GAN framework would unfavorably reduce the privacy level at each iteration, whereas we seek an approach that is free of such constraint in this paper. An interesting direction of future work is implementing the critic and seeking a privacy-utility trade-off sweet spot with privacy budget allocated optimally between training the critic and sanitizing the CF under DP.

**Data Synthesis with DP.** A significant portion of studies in the literature has been focusing on computing the output of certain algorithm or query (count, mean) under DP [32, 46, 19, 51]. They are of little relevance to the current work which takes the data synthesis approach. Traditional methods of synthesizing data are mainly concerned with discrete data or data preprocessed to the discrete form [50, 38, 8], whereas we are interested in more general methods involving continuous data. Deep generative models under the DP setting have garnered attention recently [41, 40, 47, 42, 15, 49, 7, 18]. For VAEs, the training of both the encoder and the decoder must be privatized as they interact with the data directly. In the GAN framework, while one can train the generator non-privately as the generator does not have access to the data, the discriminator interacting directly with the data must be trained privately. The private training of deep generative models is usually performed using DP-SGD. One exception is the PATE-GAN [49], which is based on the Private Aggregation of Teacher Ensembles (PATE) [35].

In DP-MERF [18], random features used to approximate the maximum mean discrepancy (MMD) objective are privatized and utilized for training a generator. PEARL, which, as a realization, uses CFs, may be viewed as a generalization of DP-MERF. Additionally, PEARL has several distinctive features which are lacking in DP-MERF. The first lies in the introduction of a privacy-preserving critic, which leads to an improvement of performance. The second is the private selection of the parameter of the sampling distribution, which is also shown to be vital. Moreover, DP-MERF uses non-characteristic kernels when treating tabular data, in contrast to ours, which is characteristic and has guarantees in convergence.

## B Additional Definitions and Previous Results

**Definition 5** (Rényi differential privacy). *A randomized mechanism  $\mathcal{M}$  is said to satisfy  $\epsilon$ -Rényi differential privacy of order  $\lambda$ , when*

$$D_\lambda(\mathcal{M}(d) \parallel \mathcal{M}(d')) = \frac{1}{\lambda - 1} \log \mathbb{E}_{x \sim \mathcal{M}(d)} \left[ \left( \frac{\Pr[\mathcal{M}(d) = x]}{\Pr[\mathcal{M}(d') = x]} \right)^{\lambda - 1} \right] \leq \epsilon$$

*is satisfied for any adjacent datasets  $d$  and  $d'$ . Here,  $D_\lambda(P \parallel Q) = \frac{1}{\lambda - 1} \log \mathbb{E}_{x \sim Q}[(P(x)/Q(x))^\lambda]$  is the Rényi divergence. Furthermore, a  $\epsilon$ -RDP mechanism of order  $\lambda$  is also  $(\epsilon + \frac{\log 1/\delta}{\lambda - 1}, \delta)$ -DP.*

Next, we note that the Gaussian mechanism is  $(\lambda, \frac{\lambda \Delta_2^2 f^2}{2\sigma^2})$ -RDP [30]. The particular advantage of using RDP is that it gives a convenient way of tracking the privacy costs when a sequence of mechanisms is applied. More precisely, the following theorem holds [30]:

**Theorem 4 (RDP Composition).** *For a sequence of mechanisms  $M_1, \dots, M_k$  s.t.  $M_i$  is  $(\lambda, \varepsilon_i)$ -RDP  $\forall i$ , the composition  $M_1 \circ \dots \circ M_k$  is  $(\lambda, \sum_i \varepsilon_i)$ -RDP.*

## C Proofs

### C.1 Proof of Thm. 2

Let  $\mathbb{P}_r$  denote the real data distribution,  $\mathbb{Q}_\theta$  denote the data distribution generated by  $G_\theta$  using a latent vector,  $z$  sampled from a pre-determined distribution, and  $\omega$  a sampling distribution.  $|\cdot|$  denotes the modulus of  $\cdot$ . Then, the CFD between the distributions is

$$\mathcal{C}_\omega^2(\mathbb{P}_r, \mathbb{Q}_\theta) = \mathbb{E}_{\mathbf{t} \sim \omega(\mathbf{t})} \left[ |\Phi_{\mathbb{P}_r}(\mathbf{t}) - \Phi_{\mathbb{Q}_\theta}(\mathbf{t})|^2 \right],$$

where  $\Phi_{\mathbb{P}}(\mathbf{t}) = \mathbb{E}_{\mathbf{x} \sim \mathbb{P}} [e^{it \cdot \mathbf{x}}]$  is the CF of  $\mathbb{P}$ . For notational brevity, we write  $\Phi_{\mathbb{P}_r}(\mathbf{t})$  as  $\Phi_r(\mathbf{t})$ , and  $\Phi_{\mathbb{Q}_\theta}(\mathbf{t})$  as  $\Phi_\theta(\mathbf{t})$  in the following.

We consider the optimized CFD,  $\sup_{\omega \in \Omega} \mathcal{C}_\omega^2(\mathbb{P}_r, \mathbb{Q}_\theta)$ , and would like to show that it is locally Lipschitz,

<sup>5</sup> which subsequently means that it is continuous. Since the Radamacher's theorem [14] implies that any locally Lipschitz function is differentiable almost everywhere, the claim of differentiability is also justified once the Lipschitz locality is proven.

We first note that the difference of two maximal functions' values is smaller or equal to the maximal difference of the two functions. Then, for any  $\theta$  and  $\theta'$ ,

$$\left| \sup_{\omega \in \Omega} \mathcal{C}_\omega^2(\mathbb{P}_r, \mathbb{Q}_\theta) - \sup_{\omega \in \Omega} \mathcal{C}_\omega^2(\mathbb{P}_r, \mathbb{Q}_{\theta'}) \right| \leq \sup_{\omega \in \Omega} \left| \mathcal{C}_\omega^2(\mathbb{P}_r, \mathbb{Q}_\theta) - \mathcal{C}_\omega^2(\mathbb{P}_r, \mathbb{Q}_{\theta'}) \right|. \quad (13)$$

We note that the absolute difference of any two complex values represented in terms of its real-number amplitude  $(A, B)$  and phase  $(\alpha, \beta)$  satisfies  $|Ae^{i\alpha} - Be^{i\beta}| \leq |A| + |B|$ . Writing the maximal  $\omega$  as  $\omega^*$ , the RHS of Eq. 13 can be written as

$$\begin{aligned} & \left| \mathcal{C}_{\omega^*}^2(\mathbb{P}_r, \mathbb{Q}_\theta) - \mathcal{C}_{\omega^*}^2(\mathbb{P}_r, \mathbb{Q}_{\theta'}) \right| \quad (14) \\ &= \mathbb{E}_{\mathbf{t} \sim \omega^*(\mathbf{t})} [(\mathcal{C}_{\omega^*}(\mathbb{P}_r, \mathbb{Q}_\theta) + \mathcal{C}_{\omega^*}(\mathbb{P}_r, \mathbb{Q}_{\theta'})) (\mathcal{C}_{\omega^*}(\mathbb{P}_r, \mathbb{Q}_\theta) - \mathcal{C}_{\omega^*}(\mathbb{P}_r, \mathbb{Q}_{\theta'}))] \\ &= \mathbb{E}_{\mathbf{t} \sim \omega^*(\mathbf{t})} [(|\Phi_r(\mathbf{t}) - \Phi_\theta(\mathbf{t})| + |\Phi_r(\mathbf{t}) - \Phi_{\theta'}(\mathbf{t})|)(|\Phi_r(\mathbf{t}) - \Phi_\theta(\mathbf{t})| - |\Phi_r(\mathbf{t}) - \Phi_{\theta'}(\mathbf{t})|)] \\ &\leq \mathbb{E}_{\mathbf{t} \sim \omega^*(\mathbf{t})} [(2|\Phi_r(\mathbf{t})| + |\Phi_\theta(\mathbf{t})| + |\Phi_{\theta'}(\mathbf{t})|)(|\Phi_r(\mathbf{t}) - \Phi_\theta(\mathbf{t})| - |\Phi_r(\mathbf{t}) - \Phi_{\theta'}(\mathbf{t})|)] \\ &\stackrel{(a)}{\leq} 4\mathbb{E}_{\mathbf{t} \sim \omega^*(\mathbf{t})} [|\Phi_r(\mathbf{t}) - \Phi_\theta(\mathbf{t})| - |\Phi_r(\mathbf{t}) - \Phi_{\theta'}(\mathbf{t})|] \\ &\stackrel{(b)}{\leq} 4\mathbb{E}_{\mathbf{t} \sim \omega^*(\mathbf{t})} [|\Phi_\theta(\mathbf{t}) - \Phi_{\theta'}(\mathbf{t})|], \end{aligned}$$

where we have used (a)  $|\Phi_{\mathbb{P}}| \leq 1$ , (b) triangle inequality. By interpreting a complex number as a vector on a 2D plane, and using trigonometric arguments, one can deduce that  $|e^{ia} - e^{ib}| = 2 \sin(|a - b|/2) \leq |a - b|$ . Then,

$$\begin{aligned} 4\mathbb{E}_{\mathbf{t} \sim \omega^*(\mathbf{t})} [|\Phi_\theta(\mathbf{t}) - \Phi_{\theta'}(\mathbf{t})|] &= 4\mathbb{E}_{\mathbf{t} \sim \omega^*(\mathbf{t})} \left[ |\mathbb{E}_z[e^{it \cdot G_\theta(z)}] - \mathbb{E}_z[e^{it \cdot G_{\theta'}(z)}]| \right] \quad (15) \\ &\stackrel{(c)}{\leq} 4\mathbb{E}_{\mathbf{t} \sim \omega^*(\mathbf{t})} [\mathbb{E}_z[|\mathbf{t} \cdot G_\theta(z) - \mathbf{t} \cdot G_{\theta'}(z)|]] \\ &\stackrel{(d)}{\leq} 4\mathbb{E}_{\mathbf{t} \sim \omega^*(\mathbf{t})} \mathbb{E}_z[|\mathbf{t}| \cdot |G_\theta(z) - G_{\theta'}(z)|]. \end{aligned}$$

In (c), we have also used the Jensen inequality. In (d), the Cauchy-Schwarz inequality has been applied. As we are assuming that  $G_\theta$  is a  $L(\theta, z)$ -Lipschitz function, we have

$$\mathbb{E}_{\mathbf{t} \sim \omega^*(\mathbf{t})} \mathbb{E}_z[|\mathbf{t}| \cdot |G_\theta(z) - G_{\theta'}(z)|] \leq 4\mathbb{E}_{\mathbf{t} \sim \omega^*(\mathbf{t})} [|\mathbf{t}|] \cdot \mathbb{E}_z[L(\theta, z)] \cdot |\theta - \theta'|. \quad (16)$$

Since we are also assuming that  $\mathbb{E}_{\mathbf{t} \sim \omega^*(\mathbf{t})} [|\mathbf{t}|], \mathbb{E}_z[L(\theta, z)] \leq \infty$ , we have shown that  $\sup_{\omega \in \Omega} \mathcal{C}_\omega$  is

locally Lipschitz, as required. It is therefore continuous and differentiable almost everywhere, as discussed above.  $\square$

<sup>5</sup>A function  $f$  is locally Lipschitz if there exist constants  $\delta \geq 0$  and  $M \geq 0$  such that  $|x - y| < \delta \rightarrow |f(x) - f(y)| \leq M \cdot |x - y|$  for all  $x, y$ .

## C.2 Proof of Thm. 3

We denote  $\mathbf{x}_n \sim \mathbb{P}_n$  and  $\mathbf{x} \sim \mathbb{P}$ , and  $\omega^*$  the maximal function of  $\omega$ . Notice that

$$\begin{aligned}
C_{\omega^*}^2(\mathbb{P}_n, \mathbb{P}) &= \mathbb{E}_{\mathbf{t} \sim \omega^*(\mathbf{t})} \left[ \left| \mathbb{E}_{\mathbf{x}_n} [e^{i\mathbf{t} \cdot \mathbf{x}_n}] - \mathbb{E}_{\mathbf{x}} [e^{i\mathbf{t} \cdot \mathbf{x}}] \right|^2 \right] \\
&= \mathbb{E}_{\mathbf{t} \sim \omega^*(\mathbf{t})} \left[ \left| \mathbb{E}_{\mathbf{x}_n} [e^{i\mathbf{t} \cdot \mathbf{x}_n}] - \mathbb{E}_{\mathbf{x}} [e^{i\mathbf{t} \cdot \mathbf{x}}] \right| \cdot \left| \mathbb{E}_{\mathbf{x}_n} [e^{i\mathbf{t} \cdot \mathbf{x}_n}] - \mathbb{E}_{\mathbf{x}} [e^{i\mathbf{t} \cdot \mathbf{x}}] \right| \right] \\
&\stackrel{(a)}{\leq} 2 \mathbb{E}_{\mathbf{t} \sim \omega^*(\mathbf{t})} \left[ \left| \mathbb{E}_{\mathbf{x}_n} [e^{i\mathbf{t} \cdot \mathbf{x}_n}] - \mathbb{E}_{\mathbf{x}} [e^{i\mathbf{t} \cdot \mathbf{x}}] \right| \right] \\
&\stackrel{(b)}{\leq} 2 \mathbb{E}_{\mathbf{t} \sim \omega^*(\mathbf{t})} \mathbb{E}_{\mathbf{x}_n, \mathbf{x}} \left[ |e^{i\mathbf{t} \cdot \mathbf{x}_n} - e^{i\mathbf{t} \cdot \mathbf{x}}| \right] \\
&\stackrel{(c)}{\leq} 2 \mathbb{E}_{\mathbf{t} \sim \omega^*(\mathbf{t})} [|\mathbf{t}|] \mathbb{E}_{\mathbf{x}_n, \mathbf{x}} [\|\mathbf{x}_n - \mathbf{x}\|]. \tag{17}
\end{aligned}$$

Here, (a) uses  $|Ae^{i\alpha} - Be^{i\beta}| \leq |A| + |B|$  as argued above Eq. 14; (b) uses Jensen inequality; (c) uses the argument  $|e^{ia} - e^{ib}| = 2 \sin(|a - b|/2) \leq |a - b|$ , given above Eq. 15. Then, by weak convergence equivalence [24], the RHS of Eq. 17 approaches zero as  $\mathbb{P}_n \xrightarrow{D} \mathbb{P}$ , hence proving the theorem.  $\square$

## C.3 Proof of Lemma. 1

Recall that for any two distributions,  $\omega(\mathbf{t})$ ,  $\omega_0(\mathbf{t})$  and any function  $f(\mathbf{t})$ ,

$$\begin{aligned}
\mathbb{E}_{\omega}[f(\mathbf{t})] &= \int f(\mathbf{t}) \omega(\mathbf{t}) d\mathbf{t} \\
&= \int f(\mathbf{t}) \frac{\omega(\mathbf{t})}{\omega_0(\mathbf{t})} \omega_0(\mathbf{t}) d\mathbf{t} \\
&= \mathbb{E}_{\omega_0} \left[ f(\mathbf{t}) \frac{\omega(\mathbf{t})}{\omega_0(\mathbf{t})} \right].
\end{aligned}$$

Hence,  $\mathbb{E}_{\omega(\mathbf{t})}[f(\mathbf{t})] = \mathbb{E}_{\omega_0} \left[ f(\mathbf{t}) \frac{\omega(\mathbf{t})}{\omega_0(\mathbf{t})} \right]$ . Let  $\omega^*$  be the maximal probability distribution. It is then clear that  $\widehat{\mathbb{E}}_{\omega}[f(\mathbf{t})] \rightarrow \mathbb{E}_{\omega}[f(\mathbf{t})]$  implies  $\widehat{\mathbb{E}}_{\omega_0} \left[ f(\mathbf{t}) \frac{\omega^*(\mathbf{t})}{\omega_0(\mathbf{t})} \right] \rightarrow \mathbb{E}_{\omega^*}[f(\mathbf{t})]$ , as desired.  $\square$

## D Experimental Setup of Two-sample Testing on Synthetic Data

Let us describe in more detail the experiment presented in Sec. 4.2. Data are generated from two unit-variance multivariate Gaussian distributions  $\mathbb{P}, \mathbb{Q}$ , where all dimensions but one have zero mean ( $\mathbb{P} \sim \mathcal{N}(\mathbf{0}_d, \mathbf{I}_d)$ ,  $\mathbb{Q} \sim \mathcal{N}((1, 0, \dots, 0)^\top, \mathbf{I}_d)$ ). We wish to conduct a two-sample test using the CF to distinguish between the two distributions, which gets more difficult as the dimensionality increases. We test if the null hypothesis where the samples are drawn from the same distribution is rejected.

Three sets of frequencies are considered. The number of frequencies in each set is set to 20. The first set is an “unoptimized” set of frequencies. The first dimension of all but one frequency has the value of zero. Other dimensions have values generated randomly from a zero-mean unit-variance multivariate Gaussian distribution. We denote the frequency with non-zero value in the first dimension by  $\mathbf{t}_0$  without loss of generality. A “normal” set of frequencies is also considered for comparison, where the frequencies of all dimensions are sampled randomly from a multivariate Gaussian distributions. Finally, we consider an “optimized” set of frequencies, where from the “unoptimized” set of frequencies, only  $\mathbf{t}_0$  is selected to be used for two-sample testing. In other words, we re-weight the set of frequencies such that all but  $\mathbf{t}_0$  has zero weight. 1,000 samples are generated from each of  $\mathbb{P}$  and  $\mathbb{Q}$ . We repeat the problem for 100 trials to obtain the rejection rate (and repeat the whole experiment 5 times to get the error bar).

## E More on DP Release of Auxiliary Information

Several examples of auxiliary information are given. The first is the modelling of tabular data. Continuous columns of tabular data can consist of multiple modes which may better be modelled



using Gaussian mixture models (GMMs) [48]. GMMs are trainable under DP using a DP version of the expectation-maximization algorithm [36]. Instead of using the continuous value as input to  $G_\theta$ , one can assign it to a GMM cluster it belongs to and use this as the input.

The second example deals with class imbalance. Note from the first part of Eq. 9 where the sum is over the number of instances in a certain class  $y_i$ . This means that minority classes may not be optimized appropriately when the generator is trained with respect to Eq. 10. One can consider releasing the count of each class in a DP manner [18] and re-weight the conditional CF by its class count. Note that such re-weighting is also potentially helpful in resolving the issues of unfairness (disparate accuracies in imbalanced classes) occurred when using DP-SGD [4]. We leave the detailed study to future work.

Another example is the estimate of the mean of pairwise distance, where the detailed discussion is available in Supplementary Sec. F.

## F DP Estimate of the Mean of Pairwise Distance

Median heuristic is applied widely in kernel methods applications to determine the bandwidth of the radial basis function (RBF) kernels [16]. The bandwidth is taken to be the median of all pairwise distances of data samples. Here we give a DP estimation of the mean instead as the calculation of mean is more tractable. Let  $\mathbf{x}$  be samples of a certain data distribution of dimension  $d$  and assume that the values lie in  $[0, 1]^d$ . Given  $n$  samples, there is a total of  $n(n-1)/2$  pairwise distance pairs. Then, the mean of the pairwise distance of samples is

$$\bar{D}_n(\mathbf{x}) = \frac{2}{n(n-1)} \sum_{i \neq j}^n \|\mathbf{x}_i - \mathbf{x}_j\|_2.$$

where  $\|\cdot\|_2$  indicates the Euclidean norm.

Consider a pair of neighboring datasets,  $\mathcal{D}, \mathcal{D}'$ . Without loss of generality, let  $\mathbf{x}_n \neq \mathbf{x}'_n$  and  $\mathbf{x}_i = \mathbf{x}'_i$  for  $i \neq n$ . Then, the sensitivity of  $\bar{D}_n(\mathbf{x})$  is

$$\begin{aligned} \Delta_{\bar{D}_n(\mathbf{x})} &= \max_{\mathcal{D}, \mathcal{D}'} \left\| \frac{2}{n(n-1)} \sum_{i \neq j}^n \|\mathbf{x}_i - \mathbf{x}_j\|_2 - \frac{2}{n(n-1)} \sum_{i \neq j}^n \|\mathbf{x}'_i - \mathbf{x}'_j\|_2 \right\|_2 \\ &\stackrel{(a)}{=} \frac{2}{n(n-1)} \max_{\mathcal{D}, \mathcal{D}'} \left\| \sum_{i=1}^{n-1} \|\mathbf{x}_i - \mathbf{x}_n\|_2 - \sum_{i=1}^{n-1} \|\mathbf{x}_i - \mathbf{x}'_n\|_2 \right\|_2 \\ &\stackrel{(b)}{=} \frac{2}{n(n-1)} \cdot (n-1)\sqrt{d} \\ &= \frac{2\sqrt{d}}{n}. \end{aligned}$$

In (a), we cancel out all terms unrelated to  $\mathbf{x}_n$  or  $\mathbf{x}'_n$ . In (b), we use the fact that  $\|\mathbf{x}_i - \mathbf{x}_n\|_2$  and  $\|\mathbf{x}_i - \mathbf{x}'_n\|_2$  lie in  $[0, \sqrt{d}]$ . After obtaining the sensitivity, one can then applies the Gaussian mechanism as in Eq. 6 to obtain the DP estimate of the mean of the pairwise distance of samples.

## G Training Algorithm

The pseudo-code of the proposed training algorithm is given in Algorithm 1.

## H Evaluation Metrics

We utilize evaluation metrics commonly used to evaluate GAN's performance, namely Fréchet Inception Distance (FID) [21] and Kernel Inception Distance (KID) [6]. FID corresponds to computing the Fréchet distance between the Gaussian fits of the Inception features obtained from real and fake distributions. KID is the calculation of the MMD of the Inception features between real and fake distributions using a polynomial kernel of degree 3.

---

**Algorithm 1:** PEARL Training

---

**Input:** Sensitive data  $\{\mathbf{x}\}_{i=1}^n$ , differential privacy noise scale  $\sigma_{\text{DP}}$ , number of frequencies  $k$ , base sampling distribution variance  $\sigma_0$ , training iterations  $T$ , learning rates  $\eta_C$  and  $\eta_G$ , number of generator iterations per critic iteration  $n_{\text{gen}}$ , batch size  $B$ , latent distribution  $P_z$

**Output:** Differentially private generator  $G_\theta$

- 1 Obtain auxiliary information (e.g., base sampling distribution variance  $\sigma_0$ );
- 2 Sample frequencies  $\{\mathbf{t}\}_{i=1}^k$  with  $\mathbf{t} \sim \mathcal{N}(\mathbf{0}, \text{diag}(\sigma_0))$ ;
- 3 **for**  $i$  **in**  $\{1, \dots, k\}$  **do**
- 4      $\hat{\Phi}_{\mathbb{P}}(\mathbf{t}_i) = \frac{1}{n} \sum_{j=1}^n e^{i\mathbf{t}_i \cdot \mathbf{x}_j}$
- 5      $\hat{\Phi}_{\mathbb{P}}(\mathbf{t}_i) \leftarrow \frac{1}{\sqrt{k}} \hat{\Phi}_{\mathbb{P}}(\mathbf{t}_i)$
- 6      $\tilde{\Phi}_{\mathbb{P}}(\mathbf{t}_i) = \hat{\Phi}_{\mathbb{P}}(\mathbf{t}_i) + \mathcal{N}(0, \Delta_{\hat{\Phi}(\mathbf{x})}^2 \sigma_{\text{DP}}^2 I)$
- 7 **end**
- 8 Accumulate privacy cost  $\epsilon$ ;
- 9  $\tilde{\phi}(\mathbf{x}) \leftarrow (\tilde{\Phi}_{\mathbb{P}}(\mathbf{t}_1), \dots, \tilde{\Phi}_{\mathbb{P}}(\mathbf{t}_k))^{\top}$
- 10 Initialize generator  $G_\theta$ , sampling distribution variance  $\sigma$  ;
- 11 **for**  $\text{step}$  **in**  $\{1, \dots, T\}$  **do**
- 12     **for**  $t$  **in**  $\{1, \dots, n_{\text{gen}}\}$  **do**
- 13         Sample batch  $\{\mathbf{z}_i\}_{i=1}^B$  with  $\mathbf{z}_i \sim P_z$ ;
- 14         **for**  $i$  **in**  $\{1, \dots, k\}$  **do**
- 15              $\hat{\Phi}_{\mathbb{Q}}(\mathbf{t}_i) = \frac{1}{B} \sum_{j=1}^B e^{i\mathbf{t}_i \cdot G_\theta(\mathbf{z}_j)}$
- 16              $\hat{\Phi}_{\mathbb{Q}}(\mathbf{t}_i) \leftarrow \frac{1}{\sqrt{k}} \hat{\Phi}_{\mathbb{Q}}(\mathbf{t}_i)$
- 17         **end**
- 18          $\hat{\phi}(\mathbf{z}) \leftarrow (\hat{\Phi}_{\mathbb{Q}}(\mathbf{t}_1), \dots, \hat{\Phi}_{\mathbb{Q}}(\mathbf{t}_k))^{\top}$
- 19          $\theta \leftarrow \theta - \eta_G \cdot \nabla_{\theta} \widehat{\mathcal{C}}_{\omega}^2(\tilde{\phi}(\mathbf{x}), \hat{\phi}(\mathbf{z}))$
- 20     **end**
- 21     Sample batch  $\{\mathbf{z}_i\}_{i=1}^B$  with  $\mathbf{z}_i \sim P_z$ ;
- 22     **for**  $i$  **in**  $\{1, \dots, k\}$  **do**
- 23          $\hat{\Phi}_{\mathbb{Q}}(\mathbf{t}_i) = \frac{1}{B} \sum_{j=1}^B e^{i\mathbf{t}_i \cdot G_\theta(\mathbf{z}_j)}$
- 24          $\hat{\Phi}_{\mathbb{Q}}(\mathbf{t}_i) \leftarrow \frac{1}{\sqrt{k}} \hat{\Phi}_{\mathbb{Q}}(\mathbf{t}_i)$
- 25     **end**
- 26      $\hat{\phi}(\mathbf{z}) \leftarrow (\hat{\Phi}_{\mathbb{Q}}(\mathbf{t}_1), \dots, \hat{\Phi}_{\mathbb{Q}}(\mathbf{t}_k))^{\top}$
- 27      $\sigma \leftarrow \sigma + \eta_C \cdot \nabla_{\sigma} \widehat{\mathcal{C}}_{\omega}^2(\tilde{\phi}(\mathbf{x}), \hat{\phi}(\mathbf{z}))$
- 28 **end**
- 29 **Return**  $G_\theta$

---

The precision definitions are as follows. Let  $\{\mathbf{x}_i^r\}_{i=1}^n$  be samples from the real data distribution  $\mathbb{P}_r$  and  $\{\mathbf{x}_i^\theta\}_{i=1}^m$  be samples from the generated data distribution  $\mathbb{Q}_\theta$ . The corresponding feature vectors extracted from a pre-trained network (LeNet in our case) are  $\{\mathbf{z}_i^r\}_{i=1}^n$  and  $\{\mathbf{z}_i^\theta\}_{i=1}^m$  respectively. The FID and KID are defined as

$$\text{FID}(\mathbb{P}_r, \mathbb{Q}_\theta) = \|\mu_r - \mu_\theta\|_2^2 + \text{Tr}(\Sigma_r + \Sigma_\theta - 2(\Sigma_r \Sigma_\theta)^{1/2}), \quad (18)$$

$$\begin{aligned} \text{KID}(\mathbb{P}_r, \mathbb{Q}_\theta) &= \frac{1}{n(n-1)} \sum_{i=1}^n \sum_{j=1, j \neq i}^n [\kappa(\mathbf{z}_i^r, \mathbf{z}_j^r)] \\ &\quad + \frac{1}{m(m-1)} \sum_{i=1}^m \sum_{j=1, j \neq i}^m [\kappa(\mathbf{z}_i^\theta, \mathbf{z}_j^\theta)] \\ &\quad - \frac{2}{mn} \sum_{i=1}^n \sum_{j=1}^m [\kappa(\mathbf{z}_i^r, \mathbf{z}_j^\theta)], \end{aligned} \quad (19)$$

where  $(\mu_r, \Sigma_r)$  and  $(\mu_\theta, \Sigma_\theta)$  are the sample mean & covariance matrix of the inception features of the real and generated data distributions, and  $\kappa$  is a polynomial kernel of degree 3:

$$\kappa(\mathbf{x}, \mathbf{y}) = \left( \frac{1}{d} \mathbf{x} \cdot \mathbf{y} + 1 \right)^3, \quad (20)$$

where  $d$  is the dimensionality of the feature vectors. We compute FID with 10 bootstrap resamplings and KID by sampling 100 elements without replacement from the whole generated dataset.

## I Implementation Details

**Datasets.** For MNIST and Fashion-MNIST, we use the default train subset of the `torchvision`<sup>6</sup> library for training the generator, and the default subset for evaluation. For Adult, we follow the preprocessing procedure in [18] to make the dataset more balanced by downsampling the class with the most number of samples.

**Neural networks.** The generator for image datasets has the following network architecture:

- $\text{fc} \rightarrow \text{bn} \rightarrow \text{fc} \rightarrow \text{bn} \rightarrow \text{upsamp} \rightarrow \text{relu} \rightarrow \text{upconv} \rightarrow \text{sigmoid}$ ,

where `fc`, `bn`, `upsamp`, `relu`, `upconv`, `sigmoid` refers to fully connected, batch normalization, 2D bilinear upsampling, ReLU, up-convolution, and Sigmoid layers respectively.

For tabular dataset, we use the following architecture:

- $\text{fc} \rightarrow \text{bn} \rightarrow \text{relu} \rightarrow \text{fc} \rightarrow \text{bn} \rightarrow \text{relu} \rightarrow \text{fc} \rightarrow \text{tanh/softmax}$ ,

where `tanh` and `softmax` are the Tanh and softmax layers respectively. Network output corresponding to the continuous attribute is passed through the Tanh layer, whereas network output corresponding to the categorical attribute is passed through the softmax layer, where the category with the highest value from the softmax output is set to be the generated value of the categorical attribute. We train both networks with conditional CFs as described in Sec. 3.3. For DP-MERF, we use the same architectures for fair comparisons.

**Hyperparameters.** We use Adam optimizer with learning rates of 0.01 for both the minimization and maximization objectives. Batch size is 100 (1,100) for the image datasets (tabular dataset). The number of frequencies is set to 1,000 (3,000) for MNIST and Adult (Fashion-MNIST). The training iterations are 6,000, 3,000, and 8,000 for MNIST, Fashion-MNIST, and Adult respectively.

## J Additional Results

**MNIST and Fashion-MNIST.** Fig. 5 and Fig. 6 show more enlarged images of MNIST and Fashion-MNIST at various level of  $\epsilon$ .

**Adult.** We show the detailed evaluation results using the synthetic data as training data for various scikit-learn classifiers in Table 3. The experiment (training generator, synthesizing data and testing with classifiers) is run 5 times to get the average values and errors. We also show more histogram plots for continuous and categorical attributes comparing our method with DP-MERF in Fig. 7 and Fig. 8.

---

<sup>6</sup><https://pytorch.org/vision/stable/index.html>

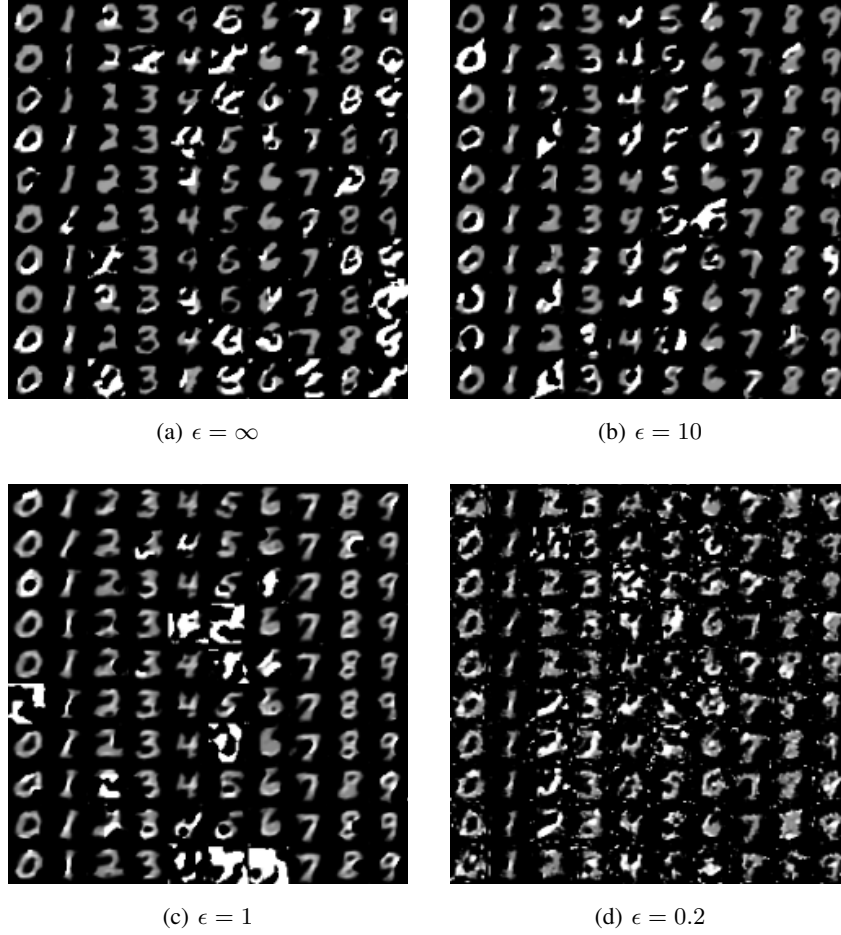
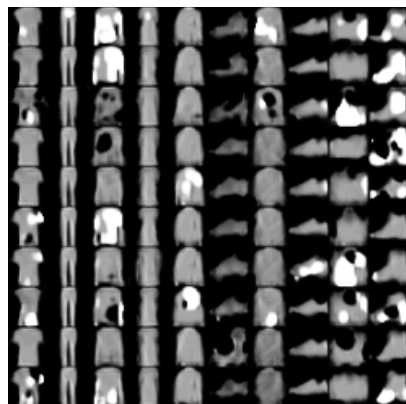


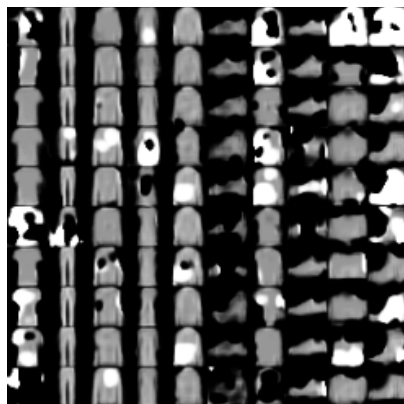
Figure 5: Additional generated MNIST images at various  $\epsilon$ .

	Real data		DP-MERF		Ours	
	ROC	PRC	ROC	PRC	ROC	PRC
LR	0.788	0.681	$0.661 \pm 0.059$	$0.542 \pm 0.041$	<b><math>0.752 \pm 0.009</math></b>	<b><math>0.641 \pm 0.015</math></b>
Gaussian NB	0.629	0.511	$0.587 \pm 0.079$	$0.491 \pm 0.06$	<b><math>0.661 \pm 0.036</math></b>	<b><math>0.537 \pm 0.028</math></b>
Bernoulli NB	0.769	0.651	$0.588 \pm 0.056$	$0.488 \pm 0.04$	<b><math>0.763 \pm 0.008</math></b>	<b><math>0.644 \pm 0.009</math></b>
Linear SVM	0.781	0.671	$0.568 \pm 0.091$	$0.489 \pm 0.067$	<b><math>0.752 \pm 0.009</math></b>	<b><math>0.640 \pm 0.015</math></b>
Decision Tree	0.759	0.646	<b><math>0.696 \pm 0.081</math></b>	$0.576 \pm 0.063$	$0.675 \pm 0.03$	<b><math>0.582 \pm 0.028</math></b>
LDA	0.782	0.670	$0.634 \pm 0.060$	$0.541 \pm 0.048$	<b><math>0.755 \pm 0.005</math></b>	<b><math>0.640 \pm 0.007</math></b>
Adaboost	0.789	0.682	$0.642 \pm 0.097$	$0.546 \pm 0.071$	<b><math>0.709 \pm 0.031</math></b>	<b><math>0.628 \pm 0.024</math></b>
Bagging	0.772	0.667	$0.659 \pm 0.06$	$0.538 \pm 0.042$	<b><math>0.687 \pm 0.041</math></b>	<b><math>0.601 \pm 0.039</math></b>
GBM	0.800	0.695	$0.706 \pm 0.069$	$0.586 \pm 0.047$	<b><math>0.709 \pm 0.029</math></b>	<b><math>0.635 \pm 0.025</math></b>
MLP	0.776	0.660	$0.667 \pm 0.088$	$0.558 \pm 0.063$	<b><math>0.744 \pm 0.012</math></b>	<b><math>0.635 \pm 0.015</math></b>

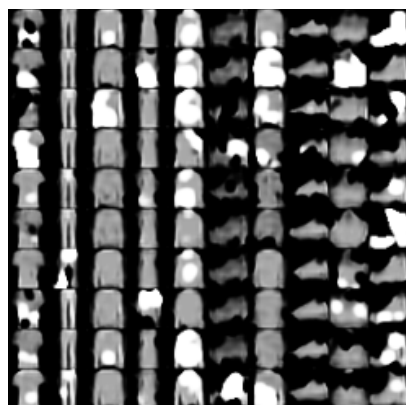
Table 3: Quantitative results for the Adult dataset evaluated at  $(\epsilon, \delta) = (1, 10^{-5})$ .



(a)  $\epsilon = \infty$



(b)  $\epsilon = 10$

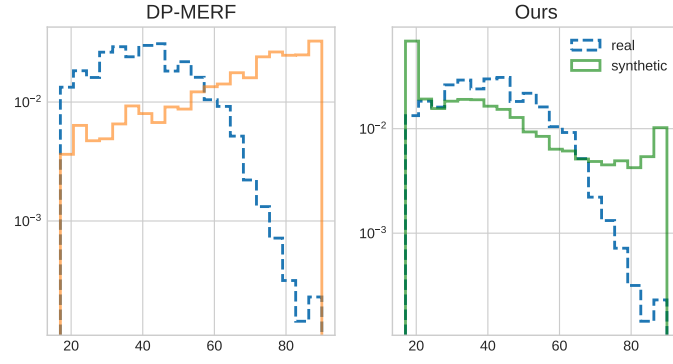


(c)  $\epsilon = 1$

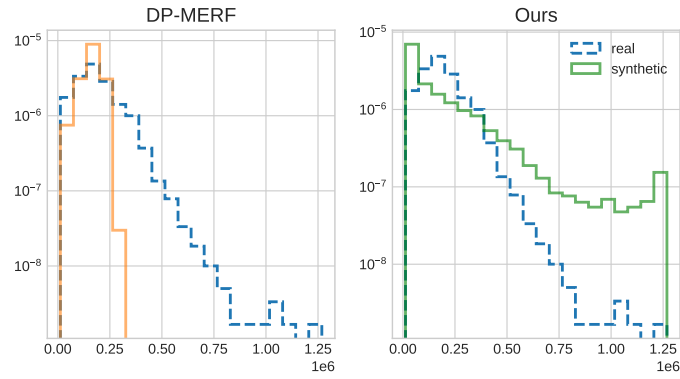


(d)  $\epsilon = 0.2$

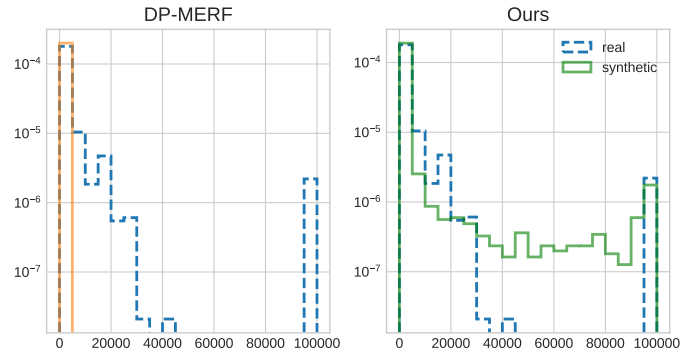
Figure 6: Additional generated Fashion-MNIST images at various  $\epsilon$ .



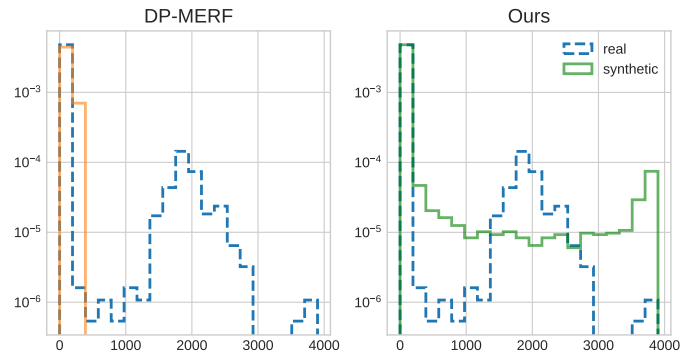
(a) Age



(b) fnlwgt



(c) Capital Gain



(d) Capital loss

Figure 7: Histograms of various continuous attributes of Adult dataset comparing real and synthetic data.

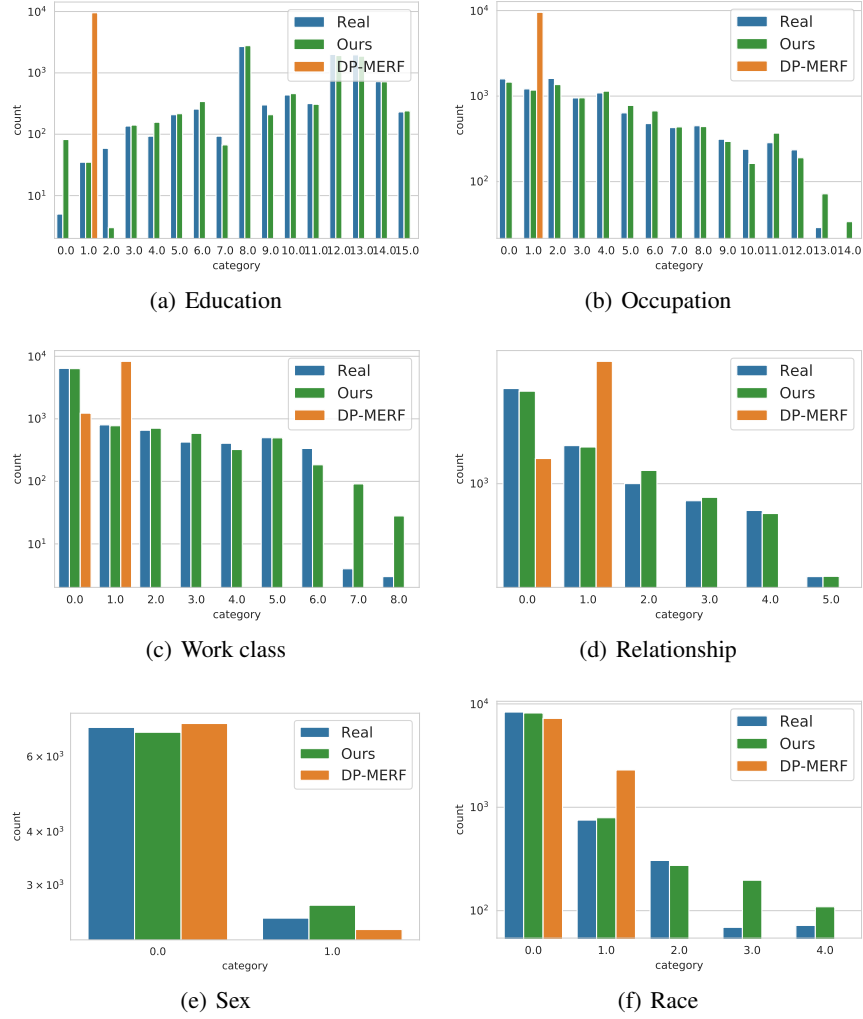


Figure 8: Histograms of various categorical attributes of Adult dataset comparing real and synthetic data.